# Influence des conditions aux limites thermiques sur la stabilisation d'une flamme laminaire pré-mélangée.

**Sandrine Berger**[1], **Florent Duchaine**[1*] **et Laurent Gicquel**[1]

[1]CERFACS, 42 avenue Gaspard Coriolis, 31 057 Toulouse
[*](auteur correspondant : florent.duchaine@cerfacs.fr)

**Résumé -** Le motif de stabilisation d'une flamme laminaire pré-mélangée pauvre sur un accroche flamme de section carrée positionné dans un canal 2D est analysée en fonction de la température du barreau. Trois grandes familles de topologies sont identifiées : des flammes décrochées se stabilisent en arrière du barreau pour les faibles températures de barreau, des flammes accroches aux parois latérales du cylindre pour les températures intermédiaires et une stabilisation de flamme en amont de l'accroche flamme pour les températures plus élevées. Ces résultats montrent un comportement non monotone de l'intégrale du flux de chaleur sur les parois du cylindre en fonction de la température pariétale, indiquant 3 valeurs de températures pouvant mener à un équilibre thermique du solide. Ces trois températures correspondent aux trois topologies de stabilisation. Finalement, des simulations de transfert de chaleur conjugué avec différentes valeurs de conductivité indiquent que deux régimes sont thermiquement stables : le premier correspond à la famille des flammes décrochées et le second pour lequel le barreau est plongé dans les gaz chauds avec une flamme stabilisée en amont.

## 1. Introduction

Aeronautical engine thermal environment is critical for efficiency and hot component lifespan. Among all the hot stream components, the combustion chamber is subject to very heterogeneous thermal fields that result from complex interactions between fresh reactants entering the chamber, turbulent combustion, flame stabilization, flow field aerodynamics and thermal mixing as well as wall thermal properties. Today, the design phase of the combustion chamber is strongly enhanced by the use of high fidelity computations. However, thermal boundary conditions are rarely well known and are thus treated mostly either as being adiabatic or at approximately fixed isothermal conditions. In many cases, the wall thermal fields have a significant impact on the reactive flows, especially through the flame stabilization process. To gain insight in the domain, this paper investigates the flame holder wall temperature influence on the flame anchoring pattern of an academic configuration : a laminar premixed flame stabilized on a squared cylinder.

Bluff-body flames rely on the introduction of an non-streamlined object in a reactive flow that creates a recirculation zone of burnt gases just downstream of the body. These recirculating hot gases constantly heat up the fresh mixture to the ignition helping the flame to maintain itself behind the obstacle. Because of their large field of application and use for academic studies or model development, bluff-body flames are widely documented in the literature. When it comes to stabilization matters, most early studies (1940s – 1950s) seek to determine flame holder stability limits ; meaning the range of fluid and/or flame holder parameters for which the flame does not blow-off [1, 2, 3]. It was shown that two parameters are of primary importance : the fresh mixture equivalence ratio and the incoming flow velocity. While early studies focus mostly on aerodynamic and chemical aspects, recent publications target to solve the Conjugate Heat Transfer (CHT) problem between the reactive flow and flame holder solid material [3, 4]. In these studies, the solid thermal properties are shown to have a significant effect on the flow

features. However, since both domains are taken into account simultaneously, one can not isolate the specific influence of the flame holder wall temperature on flame stabilization.

The present study details the variations in the stabilization pattern of a laminar premixed flame when varying a squared cylinder bluff-body wall temperature [4]. As a first step, the fluid domain is numerically solved to isolate the effect of the wall temperature on the flame anchoring patterns. Based on the these results, CHT computations with different initial temperatures of the solid body are performed to identify the effect of initial conditions on the converged thermal state.

## 2. Numerical approach

The test configuration consists of a 2D squared cylinder placed in a laminar channel flow (Fig. 1). The blocking ratio imposed to the flow by the obstacle equals $d/H = 0.2$. The inflow is a fully-developed parabolic profile prescribed with a bulk velocity equal to $U_0 = 1.6\ m.s^{-1}$. Fresh gases enter the channel at a temperature $T_0 = 300\ K$. For combustion to proceed, a perfectly premixed mixture of methane and air is injected at the inflow at an equivalence ratio of $\phi = 0.7$. The outflow condition is set at atmospheric pressure $P = 1\ atm$. The flow Reynolds number, based on the inflow quantities and the flame holder dimension, is $R_e = 500$. The low Reynolds number allows to decouple the additional complexities of flow unsteadiness and vortex shedding associated with turbulent flames.

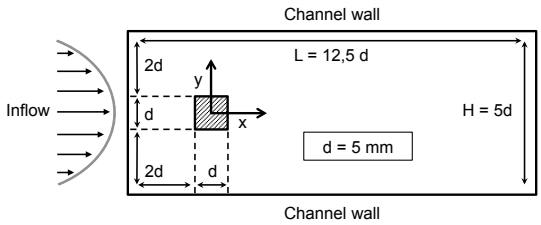


Figure 1 *Schematic view of the computationnal domain.*

The compressible reacting Navier-Stokes equations are solved on unstructured grids with the AVBP solver [5]. A second order Galerkin scheme is used for the diffusion terms [6] along with an explicit second order spatial and temporal discretization Lax Wendroff [7] scheme in a finite volume cell-vertex formalism for the convective terms. The fluid follows the ideal gas law. A multispecies formulation is used with thermodynamic properties depending both on temperature and composition. Combustion is modeled with a two-step and six species reduced kinetic scheme designed to reproduce the laminar flame speed and the adiabatic flame temperature of methane/air laminar premixed flames [8]. Both inlet and outlet are set with characteristic boundary conditions [9]. The channel walls are treated with no slip adiabatic conditions while the bluff-body walls are isothermal with the same temperature all over the surface imposed with a characteristic treatment [9].

Considering the operating conditions, the adiabatic flame temperature equals $T_{adia} = 1844\ K$ and the laminar flame speed is $S_L = 1.76 \times 10^{-1}\ m.s^{-1}$. The flame thickness based on the temperature profile is of the order of $\delta_L = 5 \times 10^{-4}$ m [10] : The mesh is accordingly refined to accurately solve the flame with a cell size of the order of $\Delta x = 96\ \mu m$. Wall mesh convergence has been checked on a baseline configuration with an isothermal bluff-body wall at $T_w = 700\ K$. The final mesh is composed of 229 354 triangles with a wall mesh size of $5 \times 10^{-5}$m leading to $y^+$ well below one on the whole body surface.

When going to CHT computations, the conduction solver AVTP is coupled to AVBP with the OpenPALM code coupler [11]. AVTP solves the heat equation with a second order Galerkin diffusion scheme [6]. Time integration is done with an implicit first order forward Euler scheme. The coupled boundaries are treated with a flux condition provided by the fluid solver. The mesh is composed of 100 $\times$ 100 square cells of size corresponding to the wall fluid cells.

## 3. Flow characteristics description of the baseline case

The flame stabilization mechanism is first detailed on the baseline case. The flow pattern is shown in Fig. 2 that depicts the temperature field along with heat release contours to visualize the flame and a zero axial velocity contour. A flame with two distinct fronts stabilizes symmetrically in the vicinity of the bluff body back corners. Additionally, a large recirculation zone encompasses the back and lateral faces of the bluff-body. The zero velocity contour slightly bends near the flame holder corners, where the flame foot stabilizes.

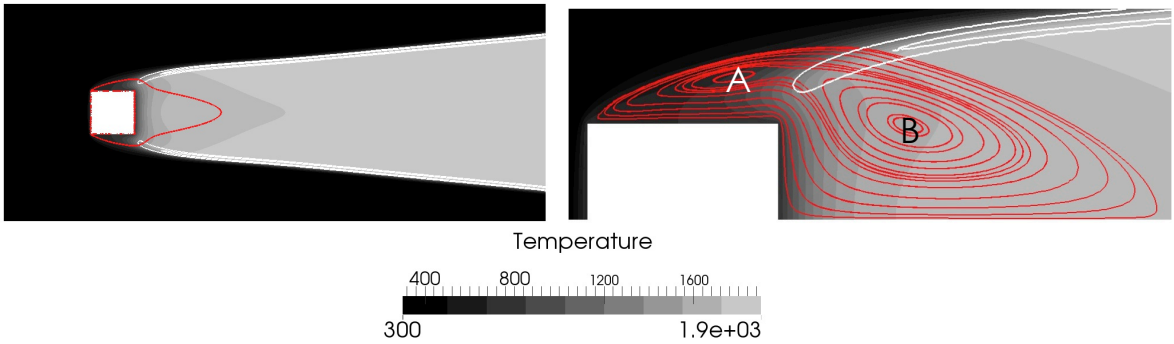


Figure 2 *Temperature field with heat release contours at* $HR = 10^8\ J.m^{-3}.s^{-1}$ *and* $HR = 10^9\ J.m^{-3}.s^{-1}$ *(white) for the baseline case* ($T_w = 700\ K$)*. Left : global view with zero axial velocity contours (red), right : zoom view with flow streamlines in the recirculation zone (red).*

The flow is composed of a recirculation zone with two kernels rotating clockwise : one located downstream of the flame holder (B on Fig. 2) and a second one near the lateral face (A). The flame foot stabilizes between the two kernels, in a region where the velocity is particularly low and hence favorable to flame development. The temperature contours near the bluff-body centerline in zone B shows a gradual cooling of the burnt gases by convection and diffusion from the cold back face of the bluff-body as the gases get closer to the wall. Near the bluff-body lateral face, in zone A, gases are warmed up both by the hot gases convected from the back and by diffusion from the hot lateral walls. Ignition temperature is thus reached thanks to the conjunction of these two warming processes. With respect to composition, the recirculation zone has a negative effect on the flame development. Indeed, it lowers the fresh gas quantity at the flame foot location by dilution with the burnt gas composition from the most downstream part B of the recirculation zone. The recirculation zone has three distinct effects : it brings hot burnt gases upstream, warming up and diluting the fresh gases and it provides a favorable aerodynamic region with very low velocity. Acting on one of these processes could affect greatly the other parameters and hence the flame stabilization pattern.

The aerodynamic field around the bluff-body as well as the temperature distribution induced by the flame stabilization pattern result in a specific wall friction and heat flux distribution along the bluff-body surface (Fig. 3). The friction velocity used here characterize the wall friction is almost similar to what can be found in the literature of laminar non-reacting bluff-body flow

configurations. Its shape is linked to the deviation of the flow as well as to the recirculation patterns. More interestingly, the wall heat flux $Q_w$ is greatly dependent on the friction velocity (Fig. 3). On the flame holder front face, the heat flux is mainly driven by the convection and a strong correlation exists with the friction velocity profile. The heat flux distribution on the lateral face is more controlled by the local temperature difference between the wall and the fresh gas, which was observed to evolve significantly with the axial coordinate in Fig. 2. As the abscissa increases, the surrounding gas temperature increases gradually from values below the wall temperature that induce a positive flux from the wall to the fluid to temperatures greatly hotter than the wall leading to a negative flux. At the bluff-body back corner ($s/d = 1.5$), the negative heat flux peaks because of the slight increase of friction velocity at that location. Finally, along the bluff-body back face, the relatively low friction velocity associated with the very high and spatially uniform temperature difference between the burnt gases and the wall lead to important negative fluxes and a rather flat profile.

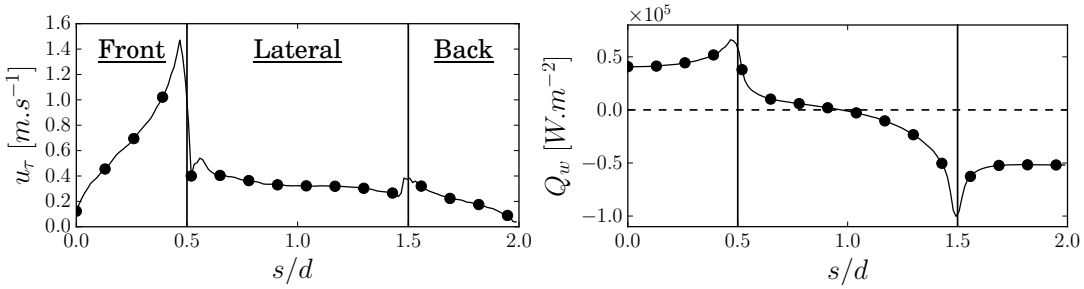


Figure 3 *Evolution of the friction velocity (left) and the wall heat flux (right) along the skin of the bluff-body top half for the baseline case.*

In this configuration, the heat exchange distribution along the bluff-body skin is controlled by both the friction and the temperature differences between the surrounding gases and the wall. These are therefore highly dependent on the local aerodynamic and thermal fields which, in the end, are coupled through the flame positioning. Since these components are strongly coupled and impact the flame stabilization pattern, a local modification of the wall temperature is expected to drastically affect the equilibrium and thereby lead to a totally different flame stabilization pattern with very different heat exchange fields. This specific point is the focus of the following section where multiple isothermal bluff-body temperature simulations are detailed.

## 4. Flame holder temperature influence

To investigate the influence of the bluff-body temperature on the flame stabilization pattern and flow fields, 15 simulations are performed for flame holder wall temperatures ranging from $T_w = 600\ K$ to $T_w = 2000\ K$ with a $100\ K$ interval between each simulation.

### 4.1. Flame stabilization and flow field variations

Figure 4 presents for each case the temperature field along with heat release contours that indicate the flame location as well as flow streamlines within the recirculation zone. The heat release contours highlight an upstream displacement of the flame foot as the wall temperature increases. As a result, the whole recirculation shape and length are modified. First, the axial length of part B of the recirculation zone decreases rapidly from approximately $2.2$ times the flame holder side length ($d$) at $T_w = 600\ K$ to $1$ at $T_w = 1000\ K$. At the latter wall temperature value, the global recirculation zone splits into two distinct zones, the lateral part (referred to

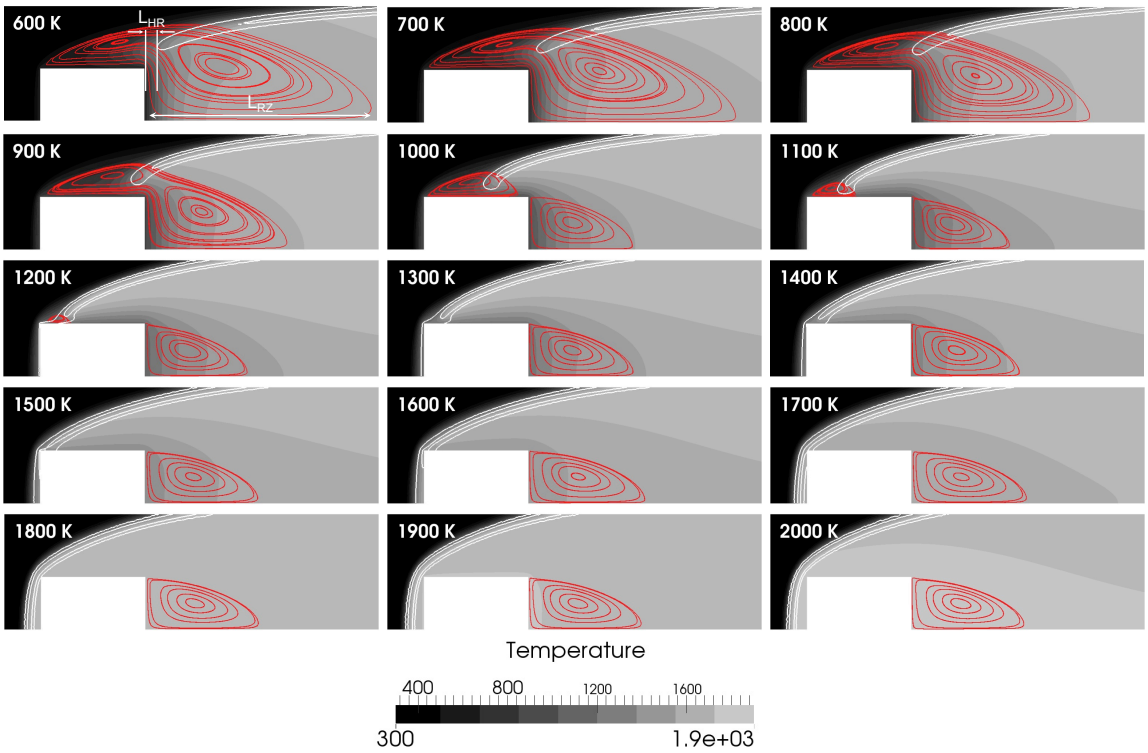


Figure 4 *Temperature field with heat release contours at* $HR = 10^8\ J.m^{-3}.s^{-1}$ *and* $HR = 10^9\ J.m^{-3}.s^{-1}$ *(white) and flow streamlines within the recirculation zone (red) in the vicinity of the flame holder on the top half of the domain.*

as zone A in Fig 2) and the downstream part B of the recirculation are no longer connected. Figure 4 indicates that above $T_w = 1000\ K$, the size of the lateral recirculation zone A reduces with increased wall temperature and eventually vanishes for $T_w = 1300\ K$. At the same time, the length of the downstream recirculation B keeps a rather constant value.

The analyzes of the flow fields allow to identify three main categories and stabilization mechanisms as a function of bluff-body wall temperature :

— $T_w \in [600; 900]\ K \rightarrow$ lifted flame : the recirculation zone plays an important role and the flame is stabilized between its two kernels,

— $T_w \in [1000; 1800]\ K \rightarrow$ anchored flame : heating of the fresh reactants by the wall are sufficient to stabilize a flame close to the lateral faces,

— $T_w \in [1900; 2000]\ K \rightarrow$ bowed flame : the flame holder is hotter than the hot products. The flame stabilizes upstream away from the cylinder.

### 4.2. Impact on the bluff body wall fluxes

The evolution of the flame stabilization pattern with wall temperature induces considerable modifications of the wall flux repartition along the bluff-body surface. These are presented in Fig. 5 on four separated plots corresponding to the main categories described previously. Focusing first on lifted flames, no clear modification of the wall heat flux distribution when varying the wall temperature is observed (Fig. 5-a) : whatever the flame holder wall temperature is, the flux evolution follows what was evidenced on the baseline case. Although the overall pattern is unaltered, flux amplitudes evolve as the wall temperature increases due to the temperature

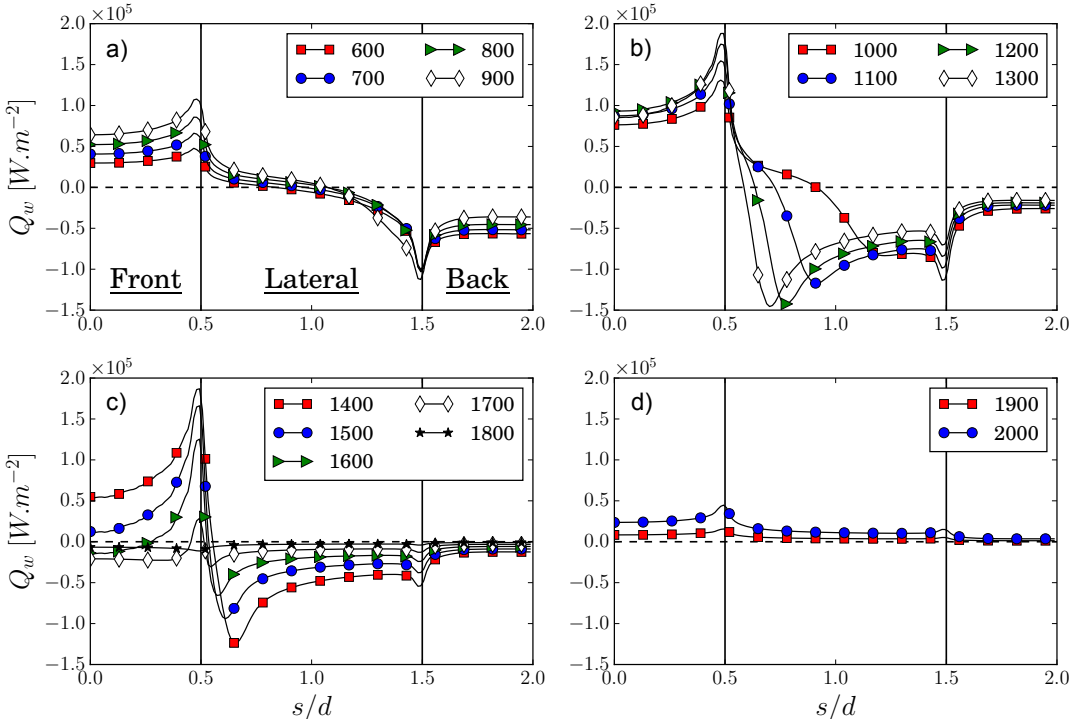


Figure 5 *Wall heat fluxes distribution along the skin of the bluff-body top half, a) for the lifted flames ($T_w \in [600; 900]\ K$), b) and c) for the anchored flames ($T_w \in [1000; 1800]\ K$) and d) for the bowed flames ($T_w \in [1900; 2000]\ K$). Fluxes are oriented towards the fluid.*

field imposed by the flame position. The heat flux shapes of the anchored flame regime is very different from the lifted one (Fig. 5-b-c). At $T_w = 1100\ K$, a clear negative peak appears at the flame foot location $s/d = 0.9$ where wall-flame interaction takes place. The walls have two antagonistic effects : first it removes energy from the flame in the classic flame-wall interaction manner but at the same time it preheats the fresh reactants, hence providing energy for the flame to be maintained. The bluff-body being entirely plunged in burnt gases, bowed flames, exhibit a rather flat flux profile along the entire flame holder walls (Fig. 5-d). Fluxes are now positive since the wall temperature is above the adiabatic flame temperature.

To investigate the influence of the flame holder wall temperature from a more global point of view, heat flux distributions are integrated separately on the front, the back and both lateral faces of the bluff-body as well as on the whole surface (Fig. 6). On the flame holder back face, integrated fluxes evolve monotonously with wall temperature, following the evolution of the temperature difference between the burnt gases and the wall. The integrated fluxes on the lateral and front faces evolve in a more complex manner. On the front face, the heat flux is first linked to the temperature difference between the wall and the fresh gases ($T_w = 600\ K$ to $T_w = 1200\ K$) and the changes due to the reaction zone developing along the bluff-body front face. The evolution of integrated fluxes on the lateral faces highlight three main behaviors as a function of the wall temperature. On the interval $T_w = [600-800]\ K$, the temperature difference between walls and the surrounding fluid decreases : negative fluxes are less and less important. Then from $T_w = 900\ K$ to $T_w = 1200\ K$, the flame interacts with the wall and gets closer to the lateral face as the wall temperature increases, creating hot areas in the vicinity of the wall and hence increasing the temperature gradients and the negative flux. Above $T_w = 1200\ K$, the flamme stabilizes upstream and takes off from the flame holder lateral face, fluxes decrease

again.

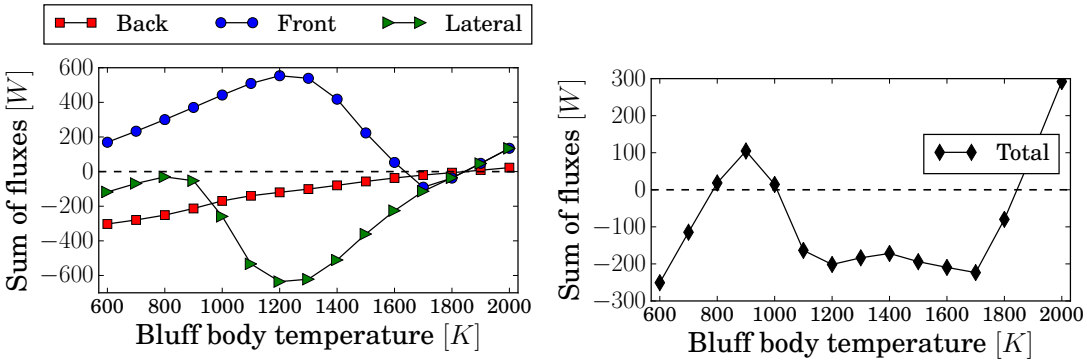


Figure 6 *Integrated fluxes along the walls of the bluff-body for the different thermal conditions.*

The integrated heat flux on the whole flame holder surface is shown in Fig. 6. The integrated flux evolves non-monotonously as a function of flame holder wall temperature. As a result, a given value of the integrated flux corresponds to various wall flux distributions and hence potentially highly different flow patterns. In particular the curve crosses the zero flux axis three times. These points are three theoretical equilibrium states and suggest that computation of a more realistic case solving conduction inside the flame holder solid part with infinite conductivity could lead to different converged results depending on the thermal initial state. Interestingly, these three equilibrium states correspond to the three regimes highlighted previously : lifted, anchored and bowed flames.

## 5. Conjugate heat transfer computations

To analyze the physical relevance of the equilibrium states outlined by the fixed temperature computations, conjugate heat transfer simulations are performed. Three conductivities of the solid medium are investigated : $\lambda_1 = 1.5\ \mathrm{Wm^{-1}K^{-1}}$, $\lambda_2 = 15\ \mathrm{Wm^{-1}K^{-1}}$ and $\lambda_3 = 150\ \mathrm{Wm^{-1}K^{-1}}$. For each conductivity, the 15 fixed temperature computations detailed previously are used as initial condition for the CHT problems resulting in a total of 45 CHT simulations : the fluid solutions are directly used as initial conditions while homogeneous temperatures are imposed in the solid domain. As illustrated in Fig. 7, the 45 CHT computations converge towards only two stable states : the lifted and bowed regimes. Depending on the conductivity, the bifurcation of convergence between these two states is in the range [900-1000] which corresponds to the transition from lifted to anchored flame regime. It appears that the anchored regime is not a physical stable regime. If the flame is too far from the solid wall, the peak heat flux identified in the wall-flame interaction regime as well as the hot burn gases on the lateral faces won't be sufficient to warm up the solid body against the convection mechanism of fresh gases. The flame will then move downstream and stabilizes as a stable lifted flame. On the other hand, the more the flame can heat up the solid body, the more the peak heat flux will be important (Fig. 5). This heating leads to an upstream propagation of the flame enlarging the hot gases region on the lateral faces until a stabilization in a bowed flame regime. Note that for lifted flames, thermal fields obtained for the three conductivities differ, leading to different mean solid temperatures, due to the difference in thermal equilibrium between the fluid and the solid.

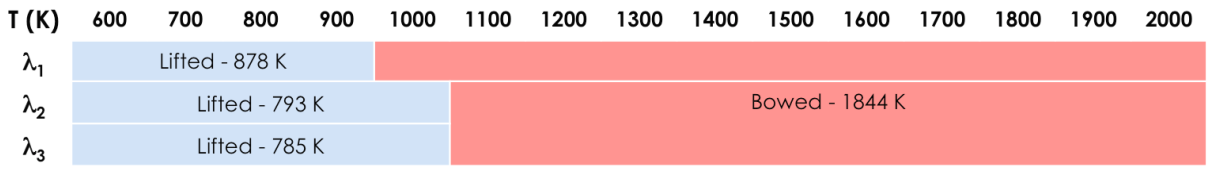


Figure 7 *Mean solid temperatures and flame regimes obtained by the 45 CHT computations.*

## 6. Conclusion

The effect of a squared cylinder flame holder wall temperature on a laminar premixed flame stabilization pattern is numerically investigated. Firstly, three flame stabilization regimes are found depending on the imposed wall temperature : lifted, anchored and bowed flames. The integrated wall heat flux around the flame holder shows a non monotonous behavior against the bluff body temperature. A thermal equilibrium state (sum of heat flux equal to zero) is obtained for three different imposed wall temperatures. These three states are potential converged solutions of conjugate heat transfer problems and interestingly correspond to the three regimes. Finally, when going to conjugate heat transfer, the computations lead to only two stable states for the different conductivities tested : lifted and bowed. Future works will investigate the role of the thermal conduction in the solid to understand the stability of the anchored regime.

**Références**

[1] G. C. Williams, C. W. Shiman, Some properties of rod-stabilized flames C homogeneous gas mixtures, Symposium (International) on Combustion 4 (1) (1953) 733–742.

[2] K. M. Kundu, D. Banerjee, D. Bhaduri, On Flame Stabilization by Bluff-Bodies, Journal of Engineering for Power 102 (1) (1980) 209–214.

[3] A. Fan, J. Wan, K. Maruta, H. Yao, W. Liu, Interactions between heat transfer, flow field and flame stabilization in a micro-combustor with a bluff body, International Journal of Heat and Mass Transfer 66 (2013) 72–79.

[4] K. S. Kedia, A. F. Ghoniem, The anchoring mechanism of a bluff-body stabilized laminar premixed flame, Combustion and Flame 161 (9) (2014) 2327–2339.

[5] T. Schønfeld, M. Rudgyard, Steady and unsteady flows simulations using the hybrid flow solver AVBP, AIAA Journal 37 (11) (1999) 1378–1385.

[6] J. Donéa, B. Roig, A. Huerta, High-order accurate time-stepping schemes for convection-diffusion problems, Comput. Methods Appl. Mech. Eng. 182 (2000) 249–275.

[7] P. Lax, B. Wendroff, Systems of conservation laws, Commun. Pure Appl. Math. 13 (1960) 217–237.

[8] B. Franzelli, E. Riber, L. Y. M. Gicquel, T. Poinsot, Large Eddy Simulation of combustion instabilities in a lean partially premixed swirled flame, Combustion and Flame 159 (2) (2012) 621–637.

[9] T. Poinsot, S. Lele, Boundary conditions for direct simulations of compressible viscous flows, J. Comput. Phys. 101 (1) (1992) 104–129.

[10] T. Poinsot, D. Veynante, Theoretical and numerical combustion, RT Edwards, Inc., 2005.

[11] F. Duchaine, S. Jauré, D. Poitou, E. Quémerais, G. Staffelbach, Thierry Morel, L. Gicquel, Analysis of high performance conjugate heat transfer with the OpenPALM coupler, Computational Science & Discovery 8 (1) (2015) 015003.